Lamb wave assessment of fiber volume fraction in composites

Michael D. Seale[a)]
Department of Physics, The College of William and Mary, Williamsburg, Virginia 23187

Barry T. Smith
Norfolk Academy, 1585 Wesleyan Drive, Norfolk, Virginia 23502

W. H. Prosser and Joseph N. Zalameda[b)]
NASA Langley Research Center, Mail Stop 231, Hampton, Virginia 23681

(Received 12 December 1997; accepted for publication 6 June 1998)

Among the various techniques available, ultrasonic Lamb waves offer a convenient method of examining composite materials. Since the Lamb wave velocity depends on the elastic properties of a material, an effective tool exists to evaluate composites by measuring the velocity of these waves. Lamb waves can propagate over long distances and are sensitive to the desired in-plane elastic properties of the material. This paper discusses a study in which Lamb waves were used to examine fiber volume fraction variations of approximately 0.40–0.70 in composites. The Lamb wave measurements were compared to fiber volume fractions obtained from acid digestion tests. Additionally, a model to predict the fiber volume fraction from Lamb wave velocity values was evaluated. © *1998 Acoustical Society of America.* [S0001-4966(98)03809-0]

PACS numbers: 43.35.Zc [HEB]

INTRODUCTION

Manufacturing anomalies such as porosity, fiber misalignment, and low fiber volume fraction can all degrade the performance of composite materials. Mechanical testing by Ghiorse[1] and Olster[2] have shown that the strength and modulus of composites exhibit a significant decrease due to porosity. The most widely used procedure for determining the fiber volume fraction and porosity content of a composite is chemical digestion. This method is destructive, only provides a local measurement, and produces toxic waste which requires disposal. Thus developing a nondestructive means of characterizing composites in order to assure the quality of the product being produced would be useful.

In past studies, thermal diffusivity measurements have shown some promise in determining porosity[3,4] and fiber volume fraction.[4,5] Eddy current measurements[6] have been used to measure fiber volume fraction in metal matrix composites and radiography[7] has been used in an effort to measure porosity. Although these techniques show promise, ultrasonics is one of the most widely accepted nondestructive techniques used to measure fiber volume fraction and porosity. Ultrasonic attenuation measurements have been used to measure porosity[3,8] and fiber volume fraction[9] and the variation of ultrasonic velocity (longitudinal and/or transverse) with both porosity[4,10–13] and fiber volume fraction[9,11–13] has been examined.

Ultrasonic Lamb waves have also been used to investigate porosity[14–16] as well as fiber volume fraction.[14,16] Lamb waves offer a convenient method of evaluating these composite materials. Since the Lamb wave velocity depends on the material properties of a structure, an effective tool exists to monitor composites by measuring the velocity of these waves. Additionally, Lamb wave measurements are better than conventional through-the-thickness ultrasonic measurements because they can propagate over long distances and are sensitive to the desired in-plane elastic properties of the material.

The following sections describe an experimental study which uses Lamb waves to nondestructively assess fiber volume fraction in composites. Previous studies by Balasubramaniam and Rose[16] successfully used higher order Lamb modes to investigate both porosity and fiber volume fraction. In this work, the velocity of the extensional mode is measured for composite samples with various fiber volume fractions. The results are also related to a model and the model is used to predict the fiber volume fraction from the velocity measurements.

I. SAMPLES

The composite samples studied were T300/934 carbon/epoxy with stacking sequences of $[0/90]_{4S}$ and $[0/90]_{8S}$. The fiber volume fractions had values ranging from approximately 0.40 to 0.70. The samples were cured in a mechanical press in an attempt to achieve consistent thickness. In order to attain 0.65 and 0.70 fiber volume fractions, the plies for these samples were prebled prior to final curing. The samples were cut from a 30.5-cm × 30.5-cm plate and had dimensions of 15.2 cm by 15.2 cm. The thicknesses, obtained by averaging ten measurements for each sample, decreased with increasing fiber volume fraction. Specimens were taken in three different areas of the large plate and chemical digestion tests were done to determine the average fiber volume fraction. According to ASTM standards,[17] the values for fiber volume fraction obtained from digestion testing are accurate to within 2%. The results for the destructive tests are shown in Table I.

[a)]Current address: NASA Langley Research Center, Mail Stop 231, Hampton, VA 23681.
[b)]Army Research Lab, Vehicle Technology Center.

TABLE I. Destructive test results to determine fiber volume fraction (FVF).

Sample	Layers	Target FVF	Destructive FVF	Thickness (mm)
40-1	16	0.40	0.380	2.00
50-1	16	0.50	0.529	1.78
60-1	16	0.60	0.590	1.57
65-1	16	0.65	0.659	1.35
70-1	16	0.70	0.690	1.35
40-2	32	0.40	0.395	3.84
50-2	32	0.50	0.518	3.40
60-2	32	0.60	0.580	3.40
65-2	32	0.65	0.660	2.72
70-2	32	0.70	0.690	2.72

II. LAMB WAVE MODEL

For a laminated composite with the 1-axis defined as the fiber direction, the 2-axis transverse to the fibers, and the 3-axis being out of the plane of the plate, the stress–strain relationship in an individual lamina is given by[18]

$$\begin{bmatrix} \sigma_1 \\ \sigma_2 \\ \tau_6 \end{bmatrix} = \begin{bmatrix} Q_{11} & Q_{12} & 0 \\ Q_{12} & Q_{22} & 0 \\ 0 & 0 & Q_{66} \end{bmatrix} \begin{bmatrix} \epsilon_1 \\ \epsilon_2 \\ \gamma_6 \end{bmatrix}, \tag{1}$$

where σ and τ represent the normal and shear stresses, respectively, and ϵ and γ represent the normal and shear strains, respectively. The Q_{ij} are the reduced stiffness components and are defined in terms of the engineering parameters as[18]

$$\begin{aligned} Q_{11} &= E_1/(1-\nu_{12}\nu_{21}), \\ Q_{22} &= E_2/(1-\nu_{12}\nu_{21}), \\ Q_{12} &= \nu_{12}E_1/(1-\nu_{12}\nu_{21}), \end{aligned} \tag{2}$$

where E_1 and E_2 are the Young's moduli in the longitudinal and transverse directions, respectively, and ν_{12} and ν_{21} are the major and minor Poisson's ratios, respectively. The Poisson's ratios in Eq. (2) are not independent quantities and are related to each other by[18]

$$\nu_{21} = \frac{E_2}{E_1}\,\nu_{12}. \tag{3}$$

The in-plane stiffnesses for the entire plate, A_{11} and A_{22}, are obtained by integrating the Q_{ij} through the thickness of the plate. These stiffness values are defined as[19]

$$A_{ij} = \int_{-h/2}^{h/2} (Q'_{ij})_k \, dz, \quad i,j = 1,2, \tag{4}$$

where h is the plate thickness and the subscript k represents each lamina. The Q'_{ij} are the transformed stiffness coefficients which take into account the orientation of each ply with respect to the wave propagation direction and are defined as[18]

$$\begin{aligned} Q'_{11} &= m^4Q_{11} + n^4Q_{22} + 2m^2n^2Q_{12} + 4m^2n^2Q_{66}, \\ Q'_{22} &= n^4Q_{11} + m^4Q_{22} + 2m^2n^2Q_{12} + 4m^2n^2Q_{66}, \\ Q'_{12} &= m^2n^2Q_{11} + m^2n^2Q_{22} + (m^4+n^4)Q_{12} - 4m^2n^2Q_{66}, \end{aligned} \tag{5}$$

where $m = \cos(\theta)$ and $n = \sin(\theta)$. The angle θ is defined as positive for a counterclockwise rotation from the primed (laminate) axes to the unprimed (individual lamina) axes. From Eq. (5), the Q'_{ij} for the 0° and 90° laminas are given by

$$\begin{aligned} (Q'_{11})_{0\ \mathrm{deg}} &= Q_{11}, \quad (Q'_{11})_{90\ \mathrm{deg}} = Q_{22}, \\ (Q'_{22})_{0\ \mathrm{deg}} &= Q_{22}, \quad (Q'_{22})_{90\ \mathrm{deg}} = Q_{11}, \\ (Q'_{12})_{0\ \mathrm{deg}} &= Q_{12}, \quad (Q'_{12})_{90\ \mathrm{deg}} = Q_{12}. \end{aligned} \tag{6}$$

The velocity of the extensional plate mode can be related to the in-plane stiffness of a composite.[19] For propagation in the 0° and 90° directions, these stiffnesses are A_{11} and A_{22}, respectively. The extensional plate mode velocity is related to the stiffness by[19]

$$v_1 = \sqrt{\frac{A_{11}}{\rho h}} \tag{7}$$

for propagation in the 0° direction and by

$$v_2 = \sqrt{\frac{A_{22}}{\rho h}} \tag{8}$$

for propagation in the 90° direction. The values for the in-plane stiffnesses A_{11} and A_{22} can be calculated using Eqs. (2)–(6) if the engineering stiffnesses of the composite are known. If the density, ρ, and overall thickness of the plate, h, are known as well, then the extensional mode velocity in the 0° and 90° directions can be computed using Eqs. (7) and (8).

The effect of fiber volume fraction on composite lamina parameters can be derived from a simple rule of mixtures approach. The density takes the form[20]

$$\rho = \rho_f V_f + \rho_m V_m \tag{9}$$

and the elastic constants are given by[18]

$$E_1 = E_{1f}V_f + E_mV_m, \tag{10}$$

$$E_2 = \frac{E_mE_{2f}}{E_{2f}V_m + E_mV_f}, \tag{11}$$

$$\nu_{12} = \nu_{12f}V_f + \nu_mV_m, \tag{12}$$

where ρ is the density, E_1 and E_2 are the longitudinal and transverse moduli, respectively, ν_{12} is Poisson's ratio, V_f is the fiber fraction, and V_m is the matrix fraction. The f and m subscripts represent the constituent properties of the fiber and matrix, respectively, and quantities without subscripts represent the composite lamina properties.

In order to predict the composite properties as a function of fiber volume, the properties of the fiber and matrix must be obtained. The elastic modulus of the matrix was obtained from the manufacturer[21] and the density and Poisson's ratio were estimated using common matrix values found in

TABLE II. Composite material properties.

Material	ρ (kg/m^3)	E_1 (GPa)	E_2 (GPa)	ν_{12}
Matrix	1220[a]	4.14[b]	4.14[b]	0.35[a]
Fiber[c]	1770	220.6	13.79	0.20

[a]Estimated from common matrix values found in Ref. 20.
[b]Reference 21.
[c]Reference 20.

Chamis.[20] The fiber properties were obtained from Chamis.[20] The various values used in the model are compiled in Table II.

The material parameters as a function of fiber volume fraction were calculated using Eqs. (9)–(12) and the values listed in Table II. From these values, the reduced stiffnesses for an individual lamina, Q_{ij}, were calculated using Eqs. (2)–(3). The in-plane stiffnesses for the laminate, A_{11} and A_{22}, were then computed using Eqs. (4)–(6). Finally, the extensional mode velocity as a function of fiber volume fraction was determined from Eqs. (7) to (8). Due to the architecture of the laminates, the velocity in the 90° direction is identical to the velocity in the 0° direction. Also, since the in-plane stiffness, A_{ij}, is dependent on the thickness of the sample, the Lamb wave velocity is independent of sample thickness because the thickness term is canceled by the factor of h in the denominator of Eqs. (7)–(8). Therefore, the calculated velocity as a function of fiber volume fraction is representative for both the 16-ply and 32-ply samples as well as for propagation in the 0° and 90° directions.

III. LAMB WAVE MEASUREMENTS

A 0.5-mm pencil lead break (Hsu-Neilsen source) on the edge of the samples was used to excite Lamb modes in the sample over a broad range of frequencies. Breaking the lead on the edge of the plate will tend to excite extensional mode (S_0) due to the fact that this mode is dominated by in-plane motion.[19] A typical signal for a lead break on the edge of a composite is shown in Fig. 1. As can be seen from the figure, the first arrival is the faster, nondispersive extensional mode, followed by the slower, dispersive flexural mode.

The signals were received by two Panametrics model V103 1.3-cm-diam transducers with a nominal center frequency of 1.0 MHz. The transducers were placed at distances of 5.1 cm and 10.2 cm from the lead break and a coupling gel was used between the transducers and the plate. The

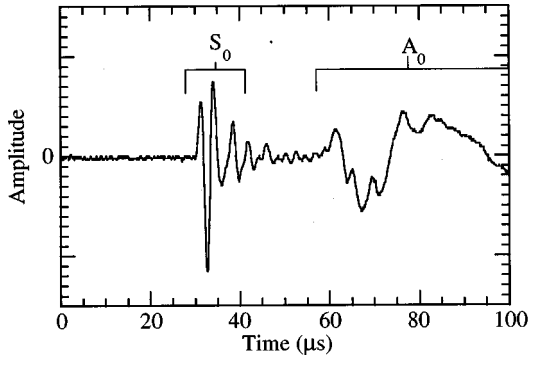

FIG. 1. Signal produced by a pencil lead break on the edge of a composite.

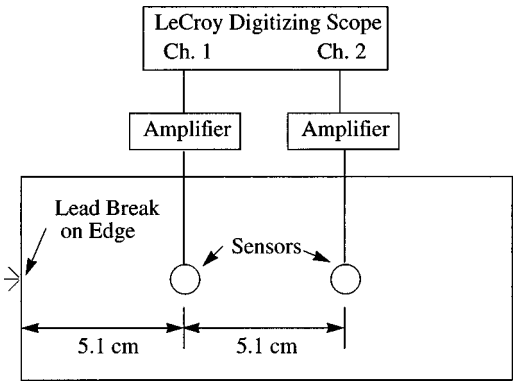

FIG. 2. Schematic showing source and receiver locations.

signals from the transducers were amplified with Tektronix AM 502 differential amplifiers and recorded on a LeCroy model 9420 digital oscilloscope. A schematic of the experimental setup is shown in Fig. 2.

The time differences were measured by imposing a delay on the first signal to overlap the signal received at a greater distance. The small thickness of the plates combined with the low-frequency Lamb wave yielded frequency-thickness products between 0.3 and 0.7 MHz·mm. In this region, only the S_0 and A_0 modes propagate (see Fig. 1). The leading part of the wave was identified as the extensional wave, which is not very dispersive. The trailing portion of the signals contained the dispersive flexural wave which was clearly separated from the extensional mode. The separation distance between the two receiving transducers was measured using a ruler and held fixed at 5.1 cm. Using the distance and time values, the velocity of the S_0 mode was measured in both the 0° and 90° directions. The final value for the velocity in each direction was obtained from the average of three measurements.

The results of the Lamb wave velocity measurements for the 16-layer samples are plotted as a function of the destructively obtained fiber volume fraction in Fig. 3. Also shown in the figure is the predicted Lamb wave velocity as a function of fiber volume fraction obtained from the model. The results for the 32-layer samples are shown in Fig. 4. The error bars represent the variation in the velocity measurements for each sample. The standard deviation for most of the specimens

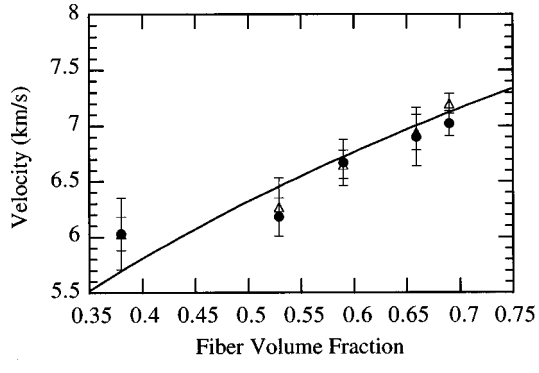

FIG. 3. Lamb wave velocity measurements in the 0° (solid circles) and 90° (open triangles) directions for the 16-layer samples. Also shown is the numerically predicted S_0 mode velocity (solid line).

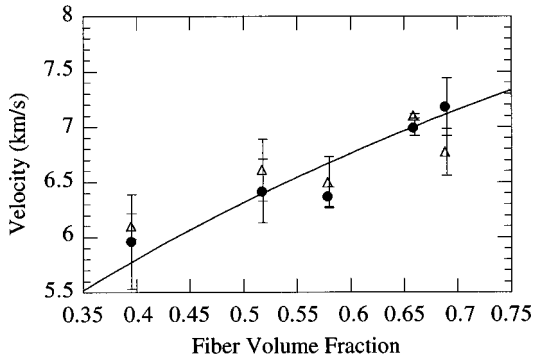

FIG. 4. Lamb wave velocity measurements in the 0° (solid circles) and 90° (open triangles) directions for the 32-layer samples. Also shown is the numerically predicted S_0 mode velocity (solid line).

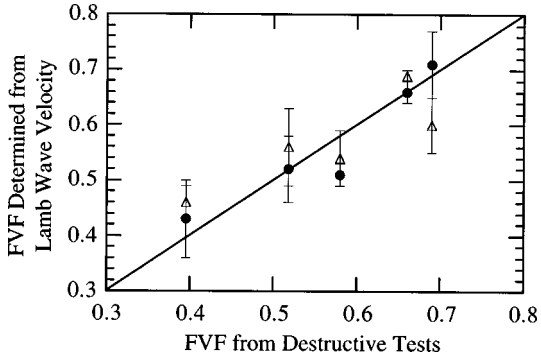

FIG. 6. Fiber volume fraction predicted using Lamb wave velocity measurements in the 0° (solid circles) and 90° (open triangles) directions compared to destructively obtained fiber volume fraction. Data are for 32-layer samples and the solid line represents an exact fit.

was less than 4% from the average of the three measurements.

Several interesting features are seen in the figures. First, the increase of the Lamb wave velocity with fiber volume fraction for both the 16-layer and 32-layer samples is quite dramatic. The increase in velocity from the 0.40 fiber volume fraction sample to the 0.70 fiber volume fraction sample is on the order of 15%. Second, due to the geometry of the samples, the velocity in the 0° and 90° directions are very similar. This is expected because the model predicts the velocities to be identical. Finally, the experimental velocities are very close to those predicted by the model. The discrepancies are probably due to the fact that the material properties used in the model were values taken from the literature. As properties of composites may vary significantly depending on cure conditions and variations in resin chemistry, the discrepancy between the actual material parameters of the manufactured composite and nominal values obtained from literature is not unexpected. Additionally, as stated earlier, there is up to a 2% error associated with the determination of fiber volume fraction from chemical digestion.[17] Therefore, the destructively obtained fiber volume fraction reported here may have some inaccuracies due to the measurement technique.

An alternate way of presenting the Lamb wave data is to use the velocity measurements to predict the fiber volume fraction. If the velocity is known, the in-plane stiffness can be calculated using Eqs. (7)–(8). From the values of A_{11} and A_{22}, the fiber volume fraction can be backed out using Eqs. (2)–(6) and Eqs. (9)–(12). The results for the 16-layer samples are shown in Fig. 5 and the results for the 32-layer samples are shown in Fig. 6. The fiber volume fraction predicted by the Lamb wave velocity measurements correlates well with the values obtained from the destructive tests. As mentioned above, the deviations seen are probably due to estimating the material properties of the system as well as manufacturing variations in the measured samples.

In addition to the Lamb wave velocity measurements, the frequency content of the S_0 mode was also examined as a function of fiber volume fraction. The average frequency from four measurements is shown in Fig. 7 for both the 16-layer and the 32-layer samples. The frequency of propagation is higher for the thin plates and the frequency increases with increasing fiber volume fraction for both the thick and the thin plates. This shift toward higher frequencies with increasing fiber fraction was demonstrated by Balasubramaniam and Rose[16] for higher order Lamb modes. Thus the frequency content as well as the Lamb wave velocity can provide useful information in characterizing the fiber volume fraction of composites.

IV. CONCLUSION

The Lamb wave velocity measurements in this study were conducted at long wavelengths. This was done for several reasons. First, if the wavelength is large compared to the

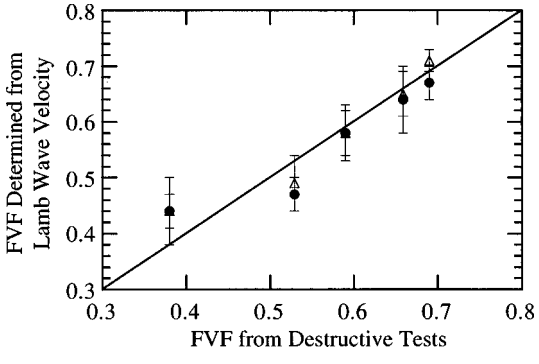

FIG. 5. Fiber volume fraction predicted using Lamb wave velocity measurements in the 0° (solid circles) and 90° (open triangles) directions compared to destructively obtained fiber volume fraction. Data are for 16-layer samples and the solid line represents an exact fit.

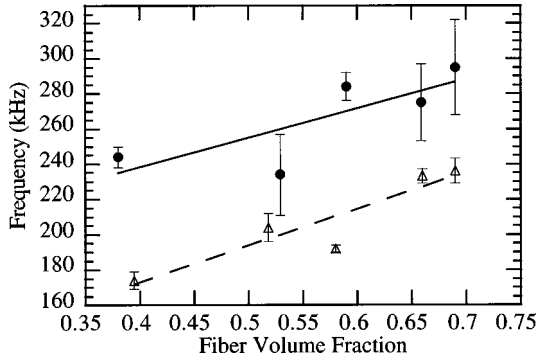

FIG. 7. Frequency versus fiber volume fraction for the 16-layer (solid circles) and 32-layer (open triangles) samples.

diameter of the fibers, composites can be treated as homogeneous. Second, only the lowest order modes propagate in the frequency range where the contact measurements were conducted. Finally, the effective elastic properties of the material can be measured because local anomalies, which scatter high frequency waves, will not be observed at long wavelengths.

Lamb waves offer a useful technique for characterizing the material properties in composite materials. Lamb wave velocity measurements are better than conventional ultrasonic measurement schemes (i.e., through-the-thickness measurements) because they can propagate over long distances and are sensitive to the desired in-plane elastic properties of the material. The propagation of Lamb waves depends on a variety of material properties: elastic stiffness constants, density, and thickness. As manufacturing abnormalities (porosity, fiber misalignment, and low fiber volume fraction) are introduced into a composite, one or more of these material properties are altered. Since the Lamb wave velocity is directly related to these parameters, a convenient method exists to monitor composites by measuring the velocity of these waves.

The Lamb wave velocity is a quantitative measurement and it has been shown by this work to be an effective tool in evaluating fiber volume fraction in composites. Thus the Lamb wave method can be used to verify the integrity of a composite after it is manufactured. This is an important measurement for flight qualified composite materials that may be used in extreme conditions. With the continued development of assessment techniques such as the Lamb wave method, the safety of such structures can be assured.

[1] S. R. Ghiorse, ''Effect of void content on the mechanical properties of carbon/epoxy laminates,'' SAMPE Quarterly **24**, 54–59 (1993).

[2] E. F. Olster, ''Effect of voids on graphite fiber reinforced composites,'' AVCO Corporation Systems Division, Final Report for U.S. Naval Air Systems Command, 1973.

[3] P. H. Johnston, W. P. Winfree, E. R. Long, Jr., S. M. Kullerd, N. Nathan, and R. D. Partos, ''Thermal and ultrasonic evaluation of porosity in composite laminates,'' in *Review of Progress in Quantitative Nondestructive Evaluation*, edited by D. O. Thompson and D. E. Chimenti (Plenum, New York, 1992), Vol. 11, pp. 1555–1562.

[4] J. N. Zalameda, ''Full field nondestructive techniques for imaging composite fiber volume fraction,'' Master's thesis, The College of William and Mary, 1996.

[5] J. N. Zalameda and W. P. Winfree, ''Quantitative thermal diffusivity measurements on composite fiber volume fraction (FVF) samples,'' in *Review of Progress in Quantitative Nondestructive Evaluation*, edited by D. O. Thompson and D. E. Chimenti (Plenum, New York, 1993), Vol. 12, pp. 1289–1295.

[6] R. E. Beissner, G. L. Burkhardt, and J. L. Fisher, ''Eddy current measurement of fiber volume fraction in metal matrix composites,'' in *Review of Progress in Quantitative Nondestructive Evaluation*, edited by D. O. Thompson and D. E. Chimenti (Plenum, New York, 1993), Vol. 12, pp. 1321–1328.

[7] B. E. Shull and J. N. Gray, ''X-Ray measurement of material properties in composites,'' in *Review of Progress in Quantitative Nondestructive Evaluation*, edited by D. O. Thompson and D. E. Chimenti (Plenum, New York, 1990), Vol. 9, pp. 1465–1471.

[8] D. K. Hsu, ''Ultrasonic measurements of porosity in woven graphite polyimide composites,'' in *Review of Progress in Quantitative Nondestructive Evaluation*, edited by D. O. Thompson and D. E. Chimenti (Plenum, New York, 1988), Vol. 7, pp. 1063–1068.

[9] H. C. Kim and J. M. Park, ''Ultrasonic wave propagation in carbon fibre-reinforced plastics,'' J. Mater. Sci. **22**, 4536–4540 (1987).

[10] D. K. Hsu and H. Jeong, ''Ultrasonic velocity change and dispersion due to porosity in composite laminates,'' in *Review of Progress in Quantitative Nondestructive Evaluation*, edited by D. O. Thompson and D. E. Chimenti (Plenum, New York, 1989), Vol. 8, pp. 1567–1573.

[11] K. Balasubramaniam, C. A. Issa, and S. Alluri, ''Ultrasonic wave propagation studies in anisotropic plates with built-in material degradation,'' in *Review of Progress in Quantitative Nondestructive Evaluation*, edited by D. O. Thompson and D. E. Chimenti (Plenum, New York, 1993), Vol. 12, pp. 1375–1382.

[12] B. G. Martin, ''Ultrasonic wave propagation in fiber-reinforced solids containing voids,'' J. Appl. Phys. **48**, 3368–3373 (1977).

[13] W. N. Reynolds and S. J. Wilkinson, ''The analysis of fibre-reinforced porous composite materials by the measurement of ultrasonic wave velocities,'' Ultrasonics **16**, 159–163 (1978).

[14] J. L. Rose, K. Balasubramaniam, J. Ditri, and A. Pilarski, ''The utility of guided waves in the ultrasonic NDE of composite materials,'' in *Non-Destructive Testing*, Proceedings of the Twelfth World Conference, Amsterdam, Netherlands, 23–28 Apr. 1989 (A91-18526 05-38) (Elsevier Science, New York, 1989), Vol. 2, pp. 1567–1572.

[15] Y. Bar-Cohen and D. E. Chimenti, ''NDE of defects in composites using leaky lamb waves,'' in *Symposium on Nondestructive Evaluation*, 15th, San Antonio, TX, 23–25 April 1985, Proceedings (A86-47129 22-38) (Nondestructive Testing Information Analysis Center, San Antonio, TX, 1986), pp. 202–208.

[16] K. Balasubramaniam and J. L. Rose, ''Guided plate wave potential for damage analysis of composite materials,'' in *Review of Progress in Quantitative Nondestructive Evaluation*, edited by D. O. Thompson and D. E. Chimenti (Plenum, New York, 1990), Vol. 9, pp. 1505–1512.

[17] D 3171-76 (Reapproved 1990) Standard Test Method for Fiber Content of Resin-Matrix Composites by Matrix Digestion, *Annual Book of ASTM Standards*, Vol. 08.01, pp. 128–130.

[18] I. M. Daniel and O. Ishai, *Engineering Mechanics of Composite Materials* (Oxford U.P., New York, 1994), pp. 3–76.

[19] W. H. Prosser, ''The propagation characteristics of the plate modes of acoustic emission waves in thin aluminum plates and thin graphite/epoxy composite plates and tubes,'' NASA Technical Memorandum 104187 (November, 1991).

[20] C. C. Chamis, ''Simplified composite micromechanics equations for hygral, thermal, and mechanical properties,'' SAMPE Quarterly **15**, 14–23 (1984).

[21] Private communication, Tom Triplett, Fiberite®, Inc.